



**HAL**  
open science

# Mid-infrared gas sensor based on high-Q/V point-defect photonic crystal nanocavities

Lazhar Kassa-Baghdouche, Eric Cassan

## ► To cite this version:

Lazhar Kassa-Baghdouche, Eric Cassan. Mid-infrared gas sensor based on high-Q/V point-defect photonic crystal nanocavities. *Optical and Quantum Electronics*, 2020, 52 (5), pp.260. 10.1007/s11082-020-02366-w . hal-04457981

**HAL Id: hal-04457981**

**<https://hal.science/hal-04457981v1>**

Submitted on 14 Feb 2024

**HAL** is a multi-disciplinary open access archive for the deposit and dissemination of scientific research documents, whether they are published or not. The documents may come from teaching and research institutions in France or abroad, or from public or private research centers.

L'archive ouverte pluridisciplinaire **HAL**, est destinée au dépôt et à la diffusion de documents scientifiques de niveau recherche, publiés ou non, émanant des établissements d'enseignement et de recherche français ou étrangers, des laboratoires publics ou privés.

# Mid-infrared gas sensor based on high-Q/V point-defect photonic crystal nanocavities

Lazhar Kassa-Baghdouche<sup>1</sup> · Eric Cassan<sup>2</sup>

## Abstract

Point-defect nanocavities based on silicon planar photonic crystal (PhC) have been optimized and studied for sensing the refractive index of gases in the mid-infrared wavelength region. The point-defect has been introduced at the center of the triangular lattice of the photonic crystal that is made up of circular air holes, making it suitable for probing the properties of the gas found within the cavity. By optimizing the radius and position of the air holes closest to the defect region precisely, on the order of a few nanometers, the ratio of the quality factor to mode volume (Q/V) for the point-defect PhC nanocavities can be increased considerably. Moreover, a perturbation method has been implemented in order to study the resonant wavelength shift of the optimized point-defect nanocavity modes caused by a small change in the refractive index of the gas. The results obtained show that sensitivity of 270 nm/RIU (Refractive Index Unit) and a detection limit of  $10^{-4}$  RIU can be achieved for the optimized point-defect PhC nanocavities. These nanocavities have been designed to oscillate at a single mode with a high Q/V thus enabling to sense the refractive index of gases with high sensitivity.

**Keywords** H1 and L3 photonic crystal nanocavities · Mid-infrared wavelength · 3D-FDTD · Perturbation theory · Refractive index gas sensing

## 1 Introduction

Over the past two decades silicon photonics technology has established silicon as an ideal substrate platform for photonic integration. Although most silicon-based photonic devices have been realized in the near-infrared (near-IR) telecommunication bands, the mid-infrared band (mid-IR), i.e. wavelength range between 2 and 20  $\mu\text{m}$ , presents a significant growth opportunity for the realization of the mid-infrared devices (Dong et al. 2017; Hu et al. 2017; Lin et al. 2017). In fact, due to the molecular fingerprints of many chemical

---

✉ Lazhar Kassa-Baghdouche  
kassabaghdouche\_lazhar@yahoo.com; kassabaghdouche.lazhar@univ-guelma.dz

<sup>1</sup> Department of Electronic and Telecommunications, Faculty of Sciences and Technology, 8 May 1945 University of Guelma, 24000 Guelma, Algeria

<sup>2</sup> Centre for Nanoscience and Nanotechnologies, CNRS UMR 9001 - Paris-Sud University, 10 Boulevard Thomas Gobert, 91120 Palaiseau, France

and biological species in their gaseous or liquid forms covered by the mid-IR wavelength range, such mid-IR band is an ideal wavelength range for the realization of the absorption-based photonic sensors (Dong et al. 2018; Chang et al. 2020). Further, such a range of the wavelength enables label-free and damage-free sensing mid-IR sensing and can utilize both changes in the real part and imaginary part of the refractive index to allow tertiary mixture sensing (Chen et al. 2014). Simultaneously, in the last few years, there has been a growing interest in photonic crystal (PhC) nanocavities due to their unique property of strong electromagnetic field confinement, small mode volume, long photon lifetime and low extinction loss. Accordingly, for sensing applications, an enhanced interaction effect gives rise to an optical mode of the PhC cavity with a resonant wavelength that is highly sensitive to the local variations in its surrounding medium. Therefore, during the last few decades, various photonic sensors composed of PhC nanocavities have been widely used in sensing applications including gases (Sünner et al. 2008; Qian et al. 2016; Zhang et al. 2015; Ge et al. 2018), solutions (Dorfner et al. 2008; Liu and Salemk 2012), bio-molecules and chemical (Kang et al. 2010; Kassa-Baghdouche 2019), electric fields (Zhao et al. 2017; Rajasekar and Robinson 2018) and nano-pressure and temperature (Rajasekar and Robinson 2019; Siraji and Zhao 2015). In addition, the effective sensing area of the PhC cavities is of the order of a micrometer or less across, which enables the integration of highly dense photonic crystal sensor arrays to realize multiplexed sensing applications (Zhou et al. 2016).

On the other hand, gas concentration measurement has always played an important role in many industrial, biomedical and environmental applications (Clerbaux et al. 2003). In order to measure and implement high-precision of low concentration gas with fast analysis time and reduced reagent consumption, there has been a growing interest in developing highly-sensitive and miniaturized optical gas sensors (Englert et al. 2014). Among them, PhC nanocavities and PhC waveguides have been designed and analyzed for the measurement of gas concentration with different refractive indices or relative gas pressures (Sünner et al. 2008; Jágerská et al. 2010; Lai et al. 2011; Zhang et al. 2013, 2015; Li et al. 2014; Qian et al. 2016; Kassa-Baghdouche and Cassan 2018; Kraeh et al. 2018; Wang et al. 2019; Vakili and Noori 2019; Maza et al. 2019). Sünner et al. (2008) studied the response of a PhC cavity to changes in the ambient refractive index. The designed heterostructure PhC cavity was formed by modulating the radii of the first row of air holes adjacent to the waveguide, which resulted in a sensitivity of 80 nm/RIU and a quality factor (Q) of 380,000. Such PhC cavities could be used to successfully identify vacuum, nitrogen, and  $SF_6$ . Besides, when the refractive index changed by  $10^{-4}$ , this led to a shift of the resonance by 8 pm when the pressure for  $SF_6$  atmosphere was changed in steps of  $0.5 \times 10^4$  Pa. Jágerská et al. (2010) improved the measurement sensitivity of measuring the refractive index of gases by introducing an air-slot in the heterostructure PhC cavities. The air-slot PhC cavity was based on a W1 waveguide with an air-slot embedded in the line-defect region. In the design, the PhC lattice was kept unchanged, but the width of the air slot was locally reduced by 20 nm to delimit the volume of the cavity. For the measurements of helium, nitrogen, and carbon dioxide, the authors have demonstrated an experimental sensitivity up to 510 nm/RIU with a detection limit higher than  $10^{-5}$  RIU. Moreover, Lai et al. (2011) demonstrated that slow light coupled with a high electric field intensity in a low-index wide slot in a silicon PhC slot waveguide device could be used to enhance the optical absorption path length. A methane concentration of 100 ppm (parts per million) in nitrogen was measured in their work. In another study, Zhang et al. (2013) proposed a high-sensitivity multi-component gas sensing system, in which the slotted PhC waveguide (SPCW) was used as the gas cell. In order to detect different kinds of gases selectively using the system, the working wavelength of the SPCW was tuned to match with one absorption line of the

gas that was being measured. In this work, a very high group index of 150 with a flat bandwidth was achieved and the electric field enhancement factor reached 12 which resulted in a minimum detection limit of 1.56 ppm. Li et al. (2014) proposed and experimentally demonstrated a series of Ln slot PhC cavities, which were operated as gas sensors. An L9 slot PhC cavity with a quality factor exceeding 30,000, sensitivity of 421 nm/RIU and a detection limit down to  $10^{-5}$  RIU was experimentally demonstrated. The simple structure and high fabrication tolerance of the proposed Ln PhC cavities extended its application in measuring different gases, such as nitrogen ( $N_2$ ), helium (He), carbon dioxide ( $CO_2$ ) and air. Zhang et al. (2015) proposed a gas concentration sensor with cryptophane E infiltrated PhC cavities. By increasing the radii of the defected holes, the proposed cavity was observed to give an RI sensitivity of 363 nm/RIU and a quality factor of the order of  $10^3$ . Besides, by combining the selective adsorption property of cryptophane E for methane and the excellent resonance property of PhC cavities, the resonant spectrum of PhC cavities was seen to sharply shift with a change in the concentration of methane gas. This resulted in a theoretical detection limit of 697 ppm for methane sensing and thus provided a new direction for the gas sensors based on PhC cavities. Qian et al. (2016) proposed a high-sensitivity gas sensing method, in which, a miniaturized PhC cavity was used as the sensing element and molecular cryptophane E was infiltrated in the defected holes of the PhC cavity as the material sensitive to methane gas. In order to enhance the RI sensitivity, a slow light PhC cavity was engineered from which a sensitivity of 450 nm/RIU and a quality factor of  $10^5$  was achieved.

Quite recently, Kassa-Baghdouche and Cassan (2018) proposed a highly efficient SPCW gas sensor working in the mid-infrared wavelength range. The transmission spectrum and sensitivity of the proposed sensor showed that a change in the refractive index of the gas by  $10^{-4}$  led to a shift of the upper band edge wavelength by 540 pm, corresponding to a sensitivity of 1720 nm/RIU. In another study, Kraeh et al. (2018) developed a gas spectrometer consisting of a microtube PhC structure. Owing to the slow light effects, the proposed structure of millimetric form factors minimizes the required absorption path length. In the design of the device, the enhanced absorption of light increased the gas sensitivity and slow-light enhanced gas absorption by a factor of 5.8 at 5400 nm. Wang et al. (2019) proposed a PhC cavity and theoretically demonstrated its possibility in tetrahydrofuran (THF) vapor sensing. In the proposed design of the PhC cavity, a portion of the air holes on both sides of the middle row was first removed to form a waveguide structure following which, two holes on both sides of the central hole were removed. By optimizing the structural parameters of several air holes, the results showed that the RI sensitivity of the proposed PhC cavity could be up to 194 nm/RIU, along with a high Q of  $2 \times 10^5$  and a detection limit as low as  $4 \times 10^{-5}$  RIU. Besides, it was theoretically verified that the PhC cavity sensor had the ability to maintain an RI sensitivity over a wide refractive index range of 1.33–1.53, enabling it to measure a larger number of parameters. Vakili and Noori (2019) proposed a 2D hole-type hexagonal lattice PhC to detect the RI change of the material infiltrated into the designed circular sensing area. In the design, the accuracy of the detection process was enhanced considering the simultaneous shift of the resonance wavelengths and the intensity modulation which occurred in two separate spectral regions. The authors showed that the structure had the ability to detect liquids, material concentrations in fluids and gases having refractive indices in the range of  $n = 1-2$  with a sensitivity of 61 nm/RIU and a quality factor of 3000. The spectroscopic detection of gases using macroporous silicon photonic crystals as narrow filters is described in another study (Maza et al. 2019). The results obtained by the authors suggest that the response of the filter for longer path lengths and higher concentrations can be predicted, showing broad working

ranges and compact sizes for CO<sub>2</sub>. Moreover, results were extrapolated to other macroporous silicon filters centered on the absorption spectra of N<sub>2</sub>O, OCS, NO<sub>2</sub>, and SO<sub>2</sub>. Heterostructure and slotted PhC nanocavities structures needed to be carefully optimized and fine-tuned in order to achieve an ultrahigh Q and low mode volumes and as a result, they had a low tolerance to fabrication deviations. Nonetheless, in order to resolve these problems and take into account the advantages of ultra-compact structure and high-sensitivity of PhC cavity-based gas sensors, it is possible to further improve the gas sensing characteristics of the point-defect PhC nanocavities with high Q/V.

With this goal, in this paper, Q/V ratio of two types of point-defect nanocavities based on planar photonic crystal is optimized, while their sensing characteristics are analyzed, to give a new perspective for further research on other gas sensing applications with such device family. The optical properties of point-defect PhC nanocavities including Q factor, mode volume, and resonant wavelength, as well as their basic sensing metrics (e.g. sensitivity, limit of detection) are computed and discussed simultaneously by the combination of three-dimensional finite difference time domain method (3D-FDTD) simulation and the perturbation theory. Firstly, in order to obtain a high sensitivity, low detection limit, and a very narrow bandwidth nanocavity mode for efficient gas sensor resolution, we have carefully maximized the ratio of the quality factor to mode volume (Q/V) and have obtained Q/V around 10<sup>5</sup>. Secondly, using the perturbation theory, the capability of the optimized point-defect PhC nanocavities to measure different gases infiltrated into air holes and claddings are demonstrated. The sensitivity characteristics of the point-defect PhC nanocavities have been optimized and their fabrication difficulty has been greatly relaxed by the chosen approach. Further, as compared to previously proposed PhC nanocavities based gas sensors, the proposed designed point-defect PhC sensors have a much simpler geometry and present higher sensitivity.

## 2 Design and modeling of PhC nanocavities

It is well known that the periodicity of the dielectric function of a photonic crystal is broken once some defects are introduced in its periodic lattice structure. This makes these structures able to guide and confine light at the scale of a few optical wavelengths. Particularly, when certain point defects are introduced in the orderly arranged lattices of PhC, it may form a PhC nanocavity surrounded by reflecting distributed boundaries. In fact, the new space created at the center of the PhC lattice supports an optical mode having a frequency located inside the photonic bandgap (PBG). Thus, for an extended number of field oscillation cycles, light can be “trapped” there, enabling strong temporal and spatial light confinements and potentially long photon lifetimes (namely, a high-quality factor) in a so-called PhC cavity (Lalanne et al. 2008).

As shown in Fig. 1, the explored point-defect planar photonic crystal cavities can be classified into two types: the H1 cavity formed by removing one lattice point in the center of the PhC lattice (Yoshie et al. 2004) and the L3 cavity formed by removing three adjacent lattice points (Chalcraft et al. 2007; Kassa-Baghdouche et al. 2014, 2015a, b, c; Kassa-Baghdouche 2019). In order to reduce the leaky components responsible for radiation losses as much as possible and thus strengthen the optical confinement within the formed dielectric resonator, the six air holes nearest to the H1 defect region and the holes at the edges of the L3 nanocavity were shifted by a distance *d*. Such displacement permits to obtain a smoother transition between the defect and PhC and can thus result in higher Q factor values and lower mode

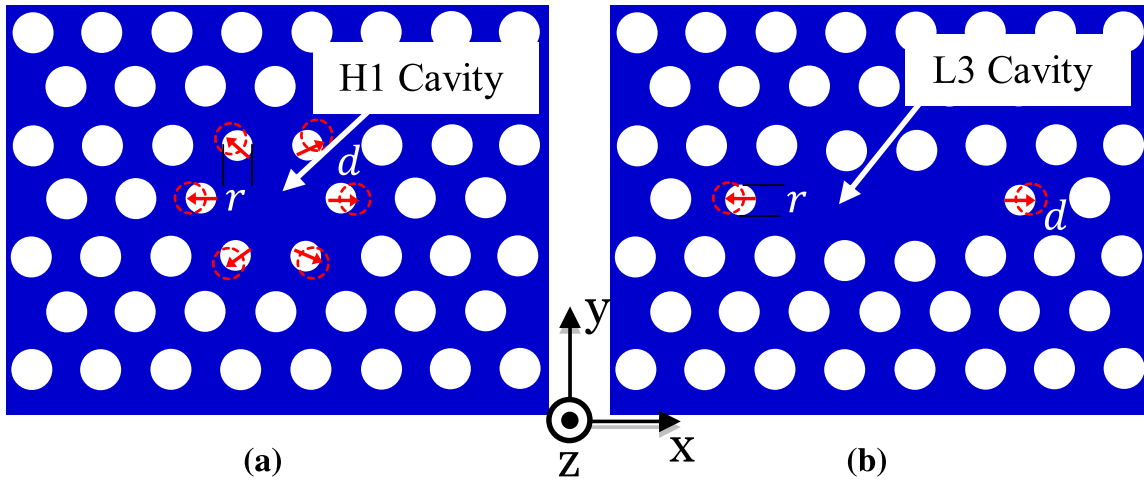


**Fig. 1** Schematic structures of two point-defect photonic crystal nanocavities. **a** H1 PhC cavity and **b** L3 PhC cavity

volumes. The L3 PhC cavity geometry has been extensively in literature and we based our work on these design guidelines (Chalcraft et al. 2007; Kassa-Baghdouche et al. 2014, 2015a, b, c; Kassa-Baghdouche 2019). The investigated structures were considered as made by air-bridge silicon PhC using a 500-nm thick silicon membrane. PhC nanocavities with triangular lattices of air holes can be fabricated using electron-beam lithography and chemically assisted ion beam etching (Yoshie et al. 2004; Chalcraft et al. 2007), and we thus considered realistic geometrical parameter values coming these studies.

In order to calculate the Q factors and mode volumes of the fundamental TE nanocavities modes, we simulated the PhC nanocavities as a 500 nm thick free standing silicon membrane ( $n = 3.42$ ) and employed the three dimensional finite difference time domain (3D-FDTD) algorithm using a modified version of a freely available MEEP software package with sub-pixel smoothing for increased accuracy (Oskooi et al. 2010). To ensure a well-confined mode, a  $17 \times 17$  lattice periods structure was used and the computational domain was bounded by perfectly matched layers (PMLs) on top and on the sides of the nanocavity surrounded by air. This PML conditions were in the calculations to ensure no back reflection in the limit of the analyzed region, but we used symmetric boundary conditions in the x- and y-directions to reduce the computing time. Nanocavities were lit by a Gaussian wave under normal incidence with a transverse electric (TE) polarized mode. The source field was placed in the middle of the nanocavity in a symmetry position for facilitate the computing of the Q factor and mode volume. To extract the resonance frequency and the cavity Q factor of the simulated structures, we used the “*harminv*” feature available in MEEP, which employs the filter diagonalization method to extract decay patterns in time series data (Mandelshtam and Taylor 1997). Our design objective was to make point-defect PhC nanocavities with resonant wavelength close to 3700 nm. For this reason, we applies a magnetic dipole source operating at a range of 3000–4000 nm.

### 3 Q/V optimization of the PhC nanocavities

In order to optimize the Q/V ratio of the proposed point-defect PhC nanocavities, by reducing unwanted reflection due to mismatch and by minimizing the propagation losses, we have performed geometrical optimization of the proposed nanocavities. The geometries of

the point-defect nanocavities studied in this work were modified by reducing the radius of the air holes closest to the defect region and then a lateral displacement ( $d$ ) of the air holes adjacent to the nanocavity was introduced (see Fig. 1). Figure 2 shows a plot of the  $Q/V$  ratio and the resonant wavelength ( $\lambda_c$ ) as a function of  $d$  for all point-defect nanocavities. As can be seen from the figure, the  $Q/V$  ratio increases with increasing  $d$  initially, owing to the strengthened optical confinement by the electric field profile, reaches a maximum and then decreases when  $d$  is greater than an optimum value. On the other hand, when the air holes are displaced too much, the electric field penetrates much beyond the displaced holes. As a result, the optical confinement occupies the space around the holes slowly, while, the electric field distribution decays abruptly outside the holes. From Fig. 2 it can be concluded that when the displacement  $d$  in the H1 PhC cavity changes by an amount as small as  $\Delta d = 10$  nm, this is enough to obtain a large increase in the  $Q/V$  ratio. For such types of nanocavities, a better result was obtained for a displacement of 85 nm, leading to  $Q/V$  of  $3.4 \times 10^4$  at the resonant wavelength  $\lambda_c = 3730$  nm.

Moreover, the plotted figure also confirms that L3 PhC nanocavities can have high  $Q/V$  values (here around  $10^5$  for a displacement of 212 nm at the resonant wavelength of  $\lambda_c = 3740$  nm). Further, we observe that an increase of the displacement  $d$  leads to a red-shift of the resonant wavelength  $\lambda_c$ , suggesting the scalability of the various designs for operation at various mid-infrared wavelengths. From this, we see that the modes of the proposed point-defect PhC nanocavities with strong electric fields in the region of the displaced holes are strongly redshifted, whereas those with minimal fields in that area are almost unaffected by end-hole displacement. We thus explain the reordering of the modes between the displacement  $d = 0a$  and  $d = 0.15a$  in terms of end-hole-field overlap. As results, this design process, based on  $3D\text{-FDTD}$  simulations, is important because we started with estimating optimum values of the displacement  $d/a$  that allow to approach the desired  $\lambda_c$  with a reasonably high  $Q/V$  value. Therefore, the above mentioned geometrical parameters are chosen in the design of the refractive gas sensor based on point-defect PhC nanocavities.

As mentioned in the above section, the lateral displacement of the air holes is an important parameter in point-defect PhC nanocavities that can be used for tuning their mode confinement condition. In the case of H1 PhC nanocavities, this displacement  $d$

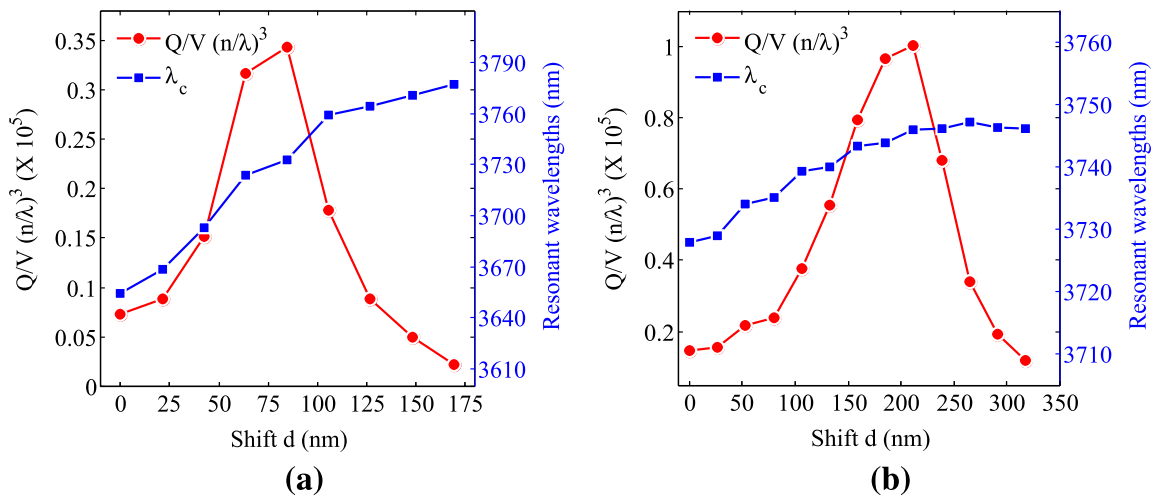


**Fig. 2** The evolution of the  $Q/V$  ratio and resonant wavelength ( $\lambda_c$ ) of the designed point-defect PhC nanocavities mode as a function of the displacement of single air holes  $d$  for reduced air-hole radii  $r' = 212$  nm. **a** H1 PhC cavity and **b** L3 PhC cavity

can be optimized because it creates space in order to confine light. On the other hand, in an L3 PhC nanocavity,  $d$  defines the confining field envelope in the cavity without a significant shift of the confined wavelengths. In other words, when a Fourier transformation of the electric field is done, the spatial change redistributes the field components in the momentum space ( $k$ -space) such that an appropriate amount of light is reflected inside the light cone ( $k < 2\pi/\lambda$ ) which might otherwise lead to out-of-plane radiation losses. This enhances the photon lifetime inside the cavity (Akahane et al. 2003). Thus, in order to further investigate the ideal method for confining light in the designed point-defect PhC nanocavity modes with optimum displacement  $d$  of the single air holes, the modal distributions of the  $E_y$  component of the fundamental mode of the designed PhC nanocavities can be analyzed using the spatial Fourier transform (FT), as shown in Fig. 3. As is evident from this figure, the electric field component  $E_y$  has an odd symmetry in the  $x$ -direction, which leads to a negligible portion of its  $K$ -vector components inside the radiation light cone. The spatial components of the leaky fields at  $K_x = 0$  are thus greatly suppressed. Furthermore, as indicated by the white circles, we can also see that the leaky components inside the light cone are reduced for optimum values of the displacement  $d$  and for the highest values of the quality factor  $Q$ . This indicates that the enhanced  $Q$  factor during the optimization process results not only from a smoother field profile but also from a more delocalized field.

#### 4 Gas sensing characteristics of the optimized PhC nanocavities

As for the sensing applications, a small variation in the local refractive index of the gases within the PhC nanocavity results in a small shift in the resonant wavelength of the nanocavity mode which is proportional to the concentration of the gas target. This phenomenon can enable the optimized point-defect PhC nanocavities to be used for the purpose of high-sensitivity gas sensing. Indeed, the spectral position,  $\lambda_c$ , of the resonant wavelength of the PhC nanocavity modes serves as a reference and the measure of the resonant wavelength shift,  $\Delta\lambda$ , is then a measure of the variation of the refractive index change  $\Delta n$  due to a

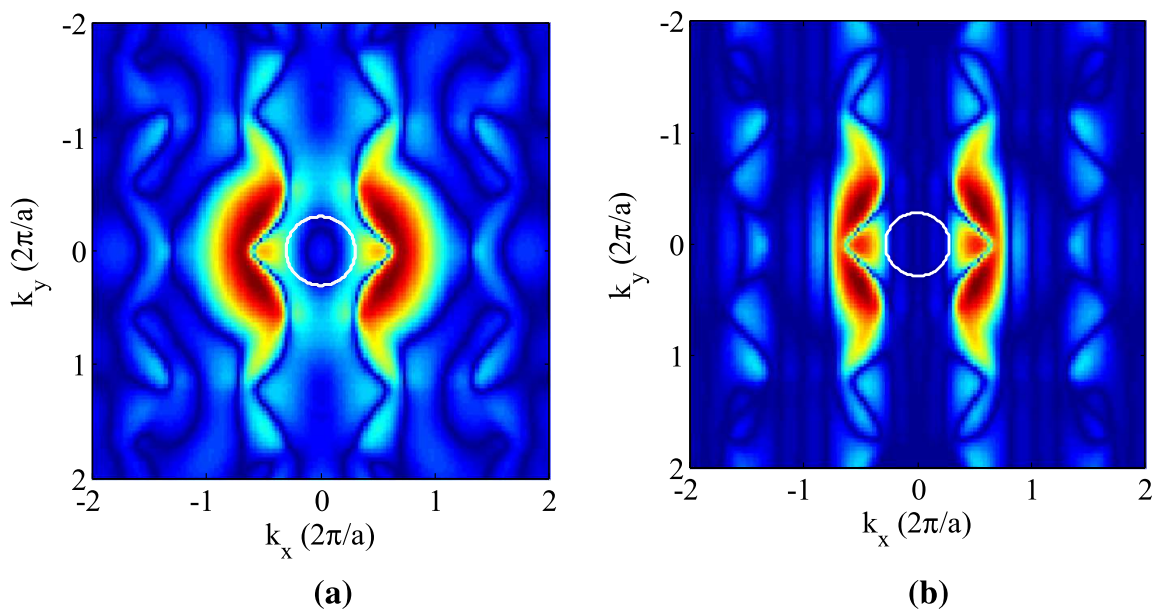


**Fig. 3** Fourier space of the  $E_y$  field distribution for the designed point-defect PhC nanocavities with optimal displacement  $d$  of single air holes. **a** H1 PhC cavity and **b** L3 PhC cavity



change in the environment of the nanocavity. The resonant frequency shift  $\Delta\lambda$  can be estimated from the electromagnetic perturbation theory for small perturbations in dielectric function,  $\Delta\epsilon$ , (Joannopoulos 2007) using:

$$\Delta\omega = \frac{-\omega \int \int \int \Delta\epsilon(\mathbf{r})|\mathbf{E}(\mathbf{r})|^2 d^3(\mathbf{r})}{2 \int \int \int \epsilon(\mathbf{r})|\mathbf{E}(\mathbf{r})|^2 d^3(\mathbf{r})} \quad (1)$$

where  $(\mathbf{E}(\mathbf{r}))$  is the electric field of the undisturbed resonant mode nanocavity. This theory shows that the variation of the resonant frequency of the nanocavity mode depends linearly on both the variation of the refractive index and the fraction of the electric field energy where the refractive index is perturbed  $\int \epsilon|\mathbf{E}(\mathbf{r})|^2$ . Therefore, any increase in the refractive index of the environment of the PhC nanocavity induces an increase in the resonant wavelength of the modes.

The evaluation of the sensitivity of the optimized point-defect PhC nanocavities can thus be done by measuring the shift of the resonant wavelength of the nanocavities modes as a function of the change of refractive index induced to the photonic crystal nanocavity environment. For a quantitative understanding of the response of optimized nanocavities to small changes in the RI of the environment, the electric field components ( $E_x, E_y$  and  $E_z$ ) were calculated using the 3D-FDTD method and perturbation theory was used to calculate small wavelength shifts for different RI of the ambient gas. Figure 4a shows the variation of the resonant wavelength shift ( $\Delta\lambda$ ) of the nanocavities modes of all optimized point-defect PhC nanocavities as a function of the refractive index of considered gases. The wavelength shift was calculated in the presence of vacuum and different gaseous environments (He, N<sub>2</sub>, CO<sub>2</sub>, C<sub>2</sub>H<sub>2</sub> and C<sub>3</sub>H<sub>8</sub>) under a pressure of 1 bar. As it can be seen from, the resonant wavelength shift indeed increases linearly with small changes in the refractive index of gases ( $n_{Gas}$ ).

Modification of the refractive index of the surrounding gas involves a variation of the index contrast between the semiconductor and the air holes. This has an influence on the effective index of the photonic crystal and its bandgap. These two effects lead to a shift of the resonant wavelength of the nanocavity modes in the same direction. That is, the resonant wavelength of the nanocavities redshift if the refractive index of gas varies from 1.000 to 1.001 and blueshift in the opposite case, namely in a case of a decrease of the gas refractive index. As the gas refractive index increases, resonance wavelength of the point-defect PhC nanocavities increases linearly. In fact, for a refractive index of gas  $n_{Gas} = 1.001$  (C<sub>3</sub>H<sub>8</sub>), a variation in the RI of the gas in the surrounding medium induces a wavelength shift of the H1 PhC nanocavity modes as little as compared to that obtained in cases of L3 nanocavities. The H1 and L3 PhC nanocavities cause a shift of 234 pm and 269 pm of cavity resonance wavelengths, respectively. Generally, gases are yet detectable by both types of cavities because their quality factors are large enough ( $\gg 10^5$ ).

By exploiting the resonant wavelength shifts estimated with the perturbation theory, the efficiency of the optimized point-defect PhC nanocavities was evaluated quantitatively by the calculation of the sensitivity  $S_\lambda = \Delta\lambda/\Delta n$  (expressed in nm/RIU) (Liu et al. 2014). This definition was chosen to characterize optimized nanocavities with respect to previous works. More quantitatively, Fig. 4b obtained in the case of the presence of different gases shows that better sensitivities can be obtained for optimized L3 nanocavity. For example, in the case of measure of the gas (C<sub>3</sub>H<sub>8</sub>), sensitivities of the optimized nanocavities are summarized in Table 1. L3 PhC cavities give higher performance compared to other optimized point-defect nanocavities. However, the sensitivity values of the optimized nanocavities remain low compared to those obtained with air slot introduced in the center of the defect

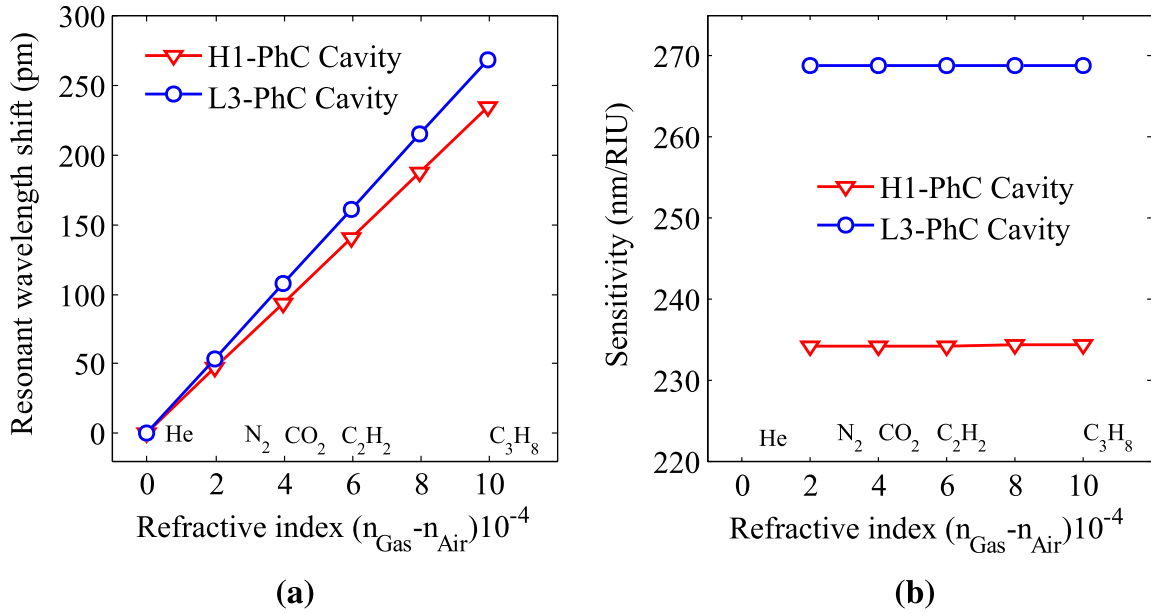


**Fig. 4** **a** Variation of resonant wavelength shift of the various point-defect PhC cavities modes as a function of the refractive indices (RI) of the gas. **b** Cavity sensitivity variation of the various point-defect PhC cavities modes as a function of the refractive indices (RI) of the gas

**Table 1** The optimum values of the Q/V ratio, sensitivity  $S_\lambda$ , detection limit DL, and resonant wavelength  $\lambda_c$  for the optimized point-defect PhC nanocavities

	Q/V	$S_\lambda$ (nm/RIU)	DL (RIU)	$\lambda_c$ (nm)
H1 PhC cavity	$1.26 \times 10^4$	234	$8.84 \times 10^{-4}$	3730
L3 PhC cavity	$10^5$	268	$1.50 \times 10^{-4}$	3740

(Li et al. 2014). This is due to the geometry of the studied slotted nanocavities, where light is strongly confined in the slot. However, for these types of the nanocavities, mode volume is smaller than for the L3 case because of the confinement of the mode in air, and thus both situations cannot be directly compared. As shown in Li et al. (2014), the confined mode electric field indeed remains much localized in the slot. However, quality factor of slotted L3 PhC nanocavities generally remains low ( $Q \sim 3 \times 10^3$ ), even by optimizing the displacement of the holes. This also testifies to the presence of a large number of field components in the cone of light. The low values of the quality factor of slotted PhC nanocavities can be explained by the abrupt termination of the slot at the holes. In this work, the low sensitivity of the optimized point-defect PhC nanocavities lies in the fact that light is well confined in the defect. This therefore makes the electric field confined in silicon.

Another way of estimating the efficiency of the optimized cavities as gas sensor devices can be performed by the calculation of the detection limit (DL) defined by:  $DL = \lambda_c / S_\lambda Q$  (expressed in RIU) (Liu et al. 2014). This parameter depends both on the sensitivity, the resonant wavelength of the nanocavity mode, and its quality factor. If the quality factor and the sensitivity of the designed PhC nanocavities increase, detection limit of the sensor increases. It brings, in addition to the sensitivity, the information of the fineness of the peak of resonance and it evolves linearly with the quality factor. So, a high Q factor improves the resolution of the resonant wavelength and thus improves the

performance of optical sensors. Table 1 summarizes the optimum values of the Q/V ratio, sensitivity  $S_\lambda$ , detection limit DL, and resonant wavelength  $\lambda_c$  for all optimized point-defect PhC nanocavities. In this study, the values of these parameters were obtained in presence of gas ( $C_3H_8$ ). We can notice that the detection limit (DL) of the optimized point-defect PhC nanocavities is of the order of  $10^4$ . This phenomenon induces a lower sensitivity which is compensated by a high quality factor.

The distribution of the electric energy density  $\epsilon|E|^2$  of the optimized point-defect PhC nanocavities is shown in Fig. 5, where the distribution profile of the electric energy density was calculated for all PhC nanocavities immersed in acetylene gas. The results show that there is an apparent difference in the distribution of  $\epsilon|E|^2$  between the optimized PhC nanocavities. For PhC nanocavities, the electric energy density distribution indicates that a substantial fraction of the energy of the confined mode is localized at the center of the defect (silicon region), which is a unique property of point-defect PhC nanocavities. However, a small energy density distribution is localized within the air holes surrounding the defect. It is worth mentioning that a small shift of the resonant wavelength of the nanocavity mode occurs even for small changes caused by the penetration depth of the field, thereby implying a much lower sensitivity. Even so, this concentration of the field in the higher refractive index region can be interesting, allowing high confinement of light in the silicon defect, for applications such as temperature sensors.

Moreover, the ratio of the quality factor to mode volume (Q/V) of the optimized point-defect PhC nanocavities has been analyzed when it is immersed in different gases. Owing to the small changes in the RI of the gas, the corresponding Q/V of the fundamental mode has been calculated and is shown in Fig. 6. As indicated in the previous section, when the RI of the gas remains unperturbed ( $n = n_o = 1.00$ ), Q/V of the optimized nanocavities is as high as  $10^4$  and  $10^5$  for H1 and L3 PhC nanocavities respectively. However, as can be seen from Fig. 6, even though the refractive index of the gas changes from 1.000 to 1.001, the Q/V ratio remains constant at a high level above  $10^4$  and  $10^5$  for the H1 and L3 PhC nanocavities respectively, indicating that the confinement of light in the proposed nanocavities is very high.

For the optimized PhC nanocavity based gas sensor, we have focused on the high-Q/V cases and small variations of the refractive index in the range of  $10^{-4}$  were used for the

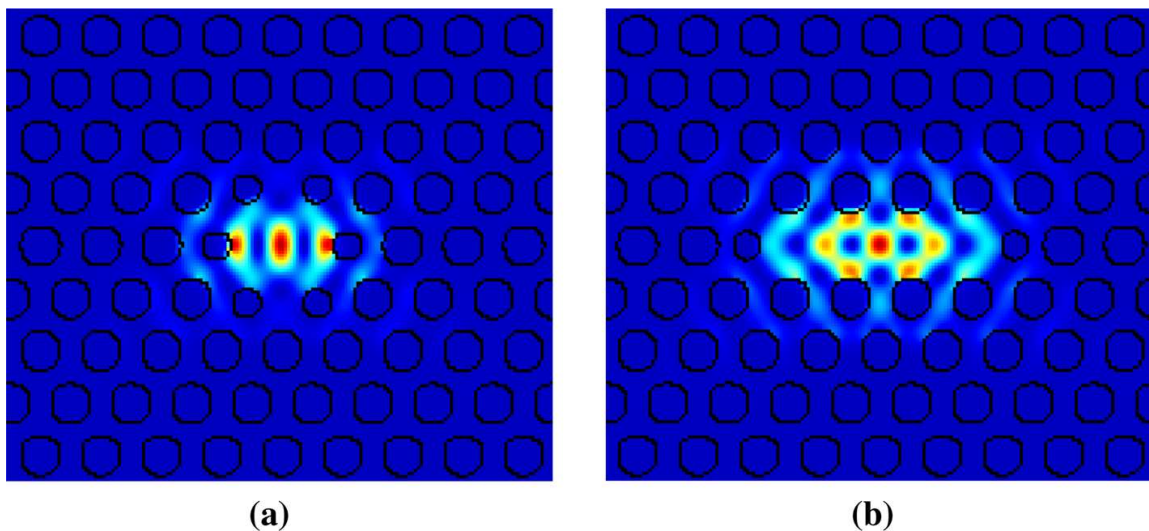
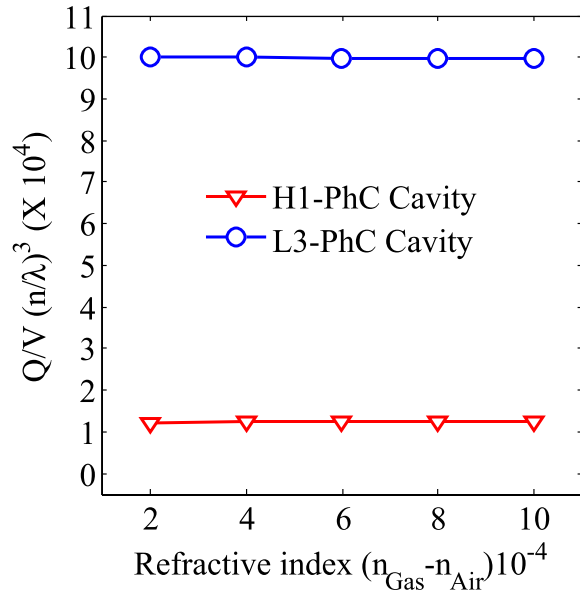


**Fig. 5** Distribution of the electric energy density  $\epsilon|E|^2$  for point-defect photonic crystal nanocavities immersed in  $C_3H_8$  gas shown in the  $x$ - $y$  plane at the optimum displacement

**Fig. 6** The variation of the Q/V ratio of the optimized point defect PhC nanocavities with background refractive index (RI)



identification of gases. From this study, it has been found that for L3 PhC nanocavity, the sensitivity was about 270 nm/RIU with a very high Q/V of  $10^4$ . However, H1 PhC cavity had a sensitivity of about 234 nm/RIU and Q/V could be up to  $10^4$ . We note that the two point-defect PhC nanocavities were chosen as the optimal designs because for gas sensor applications Q/V is crucial to gain high sensitivity. Previous studies have reported that the optimized slotted Ln PhC nanocavities have an extremely high sensitivity as well as very large light confinement in the slot (Li et al. 2014), while, the sensitivity of the improved gas sensor is higher than most of the reported results for other PhC nanocavity sensors. In addition, a measurement resolution of 1 ppm has been achieved for acetylene gas with good temperature stability. In this work, it is important to note that the sensing performance was investigated by changing the position of the air holes nearest to the defect in the direction transverse to the light propagation. In light of the literature on PhC nanocavity sensors, the 3D-Finite-Difference Time-Domain (FDTD) calculations indicated that changing the position of these holes leads to a high-Q/V. Therefore, accompanied by a proper operating wavelength around 3700 nm, our designed point-defect PhC nanocavities with high-Q/V can function as a high-sensitivity ultra-compact gas sensor used for the determination of gas traces.

## 5 Conclusion

To conclude, we have designed and simulated in this paper an efficient point-defect photonic crystal nanocavity platform for RI-based gas sensing application for wavelengths near  $\lambda_c = 3.7 \mu\text{m}$ . Results show that the Q/V ratio of the point-defect PhC nanocavities can be significantly improved with respect to previously reported results by carefully tuning a few surrounding structural parameters near the defect, i.e., by tuning the exact position of a set of two reduced air holes adjacent to the defect and their displacement in the cavity axis direction. The nanocavity with one and three missing holes has a simple design and enables maintaining a high Q/V larger than  $10^4$  and  $10^5$  for H1 and L3 PhC nanocavities respectively. From the point of view of its practical application, i.e., the sensing characteristics

of the optimized point-defect PhC nanocavities, we have studied the resonant wavelength shift, sensitivity, and detection limit characteristics of the optimized PhC nanocavities using the perturbation theory. The carried out extensive simulation results show that the optimized gas sensor is highly sensitive to a small change in refractive index of the order of  $10^{-4}$ , and a high sensitivity of 270 nm/RIU with a detection limit of  $10^{-4}$  RIU were demonstrated at  $\lambda_c = 3.7 \mu\text{m}$  for a device of  $37 \mu\text{m}$  total length. Considering the benefits of high-Q/V ratio resonators, high sensitivity, high detection limit and small sensing area, we believe that the optimized point-defect PhC nanocavities can be a suitable and useful platform for on-chip gas sensing arrays.

## References

- Akahane, Y., Asano, T., Song, B.S., Noda, S.: High-Q photonic nanocavity in a two-dimensional photonic crystal. *Nature* **425**(6961), 944–947 (2003)
- Chalcraft, A., Lam, S., O'Brien, D., Krauss, T., Sahin, M., Szymanski, D., Sanvitto, D., Oulton, R., Skolnick, M., Fox, A., et al.: Mode structure of the L3 photonic crystal cavity. *Appl. Phys. Lett.* **90**(24), 241117 (2007)
- Chang, Y., Dong, B., Ma, Y., Wei, J., Ren, Z., Lee, C.: Vernier effect-based tunable mid-infrared sensor using silicon-on-insulator cascaded rings. *Opt. Express* **28**(5), 6251–6260 (2020)
- Chen, Y., Lin, H., Hu, J., Li, M.: Heterogeneously integrated silicon photonics for the mid-infrared and spectroscopic sensing. *ACS Nano* **8**(7), 6955–6961 (2014)
- Clerbaux, C., Hadji-Lazaro, J., Turquety, S., Mégie, G., Coheur, P.F.: Trace gas measurements from infrared satellite for chemistry and climate applications. *Atmos. Chem. Phys.* **3**(5), 1495–1508 (2003)
- Dong, B., Guo, X., Ho, C.P., Li, B., Wang, H., Lee, C., Luo, X., Lo, G.Q.: Silicon-on-insulator waveguide devices for broadband mid-infrared photonics. *IEEE Photonics J.* **9**(3), 1–10 (2017)
- Dong, B., Hu, T., Luo, X., Chang, Y., Guo, X., Wang, H., Kwong, D.L., Lo, G.Q., Lee, C.: Wavelength-flattened directional coupler based mid-infrared chemical sensor using bragg wavelength in subwavelength grating structure. *Nanomaterials* **8**(11), 893–906 (2018)
- Dorfner, D., Hürlimann, T., Zabel, T., Frandsen, L.H., Abstreiter, G., Finley, J.: Silicon photonic crystal nanostructures for refractive index sensing. *Appl. Phys. Lett.* **93**(18), 181103 (2008)
- Englert, C.R., Stevens, M.H., Brown, C.M., Harlander, J.M., DeMajistre, R., Marr, K.D.: High sensitivity trace gas sensor for planetary atmospheres: miniaturized Mars methane monitor. *J. Appl. Remote Sens.* **8**(1), 083625 (2014)
- Ge, R., Xie, J., Yan, B., Liu, E., Tan, W., Liu, J.: Refractive index sensor with high sensitivity based on circular photonic crystal. *JOSA A* **35**(6), 992–997 (2018)
- Hu, T., Dong, B., Luo, X., Liow, T.Y., Song, J., Lee, C., Lo, G.Q.: Silicon photonic platforms for mid-infrared applications. *Photonics Res.* **5**(5), 417–430 (2017)
- Jágerská, J., Zhang, H., Diao, Z., Le Thomas, N., Houdré, R.: Refractive index sensing with an air-slot photonic crystal nanocavity. *Opt. Lett.* **35**(15), 2523–2525 (2010)
- Joannopoulos, J., Johnson, S., Meade, R.: *Photonic Crystals: Molding the Flow of Light*. Princeton University Press, Cambridge (2007)
- Kang, C., Phare, C.T., Vlasov, Y.A., Assefa, S., Weiss, S.M.: Photonic crystal slab sensor with enhanced surface area. *Opt. Express* **18**(26), 27930–27937 (2010)
- Kassa-Baghdouche, L.: Optical properties of a point-defect nanocavity-based elliptical-hole photonic crystal for mid-infrared liquid sensing. *Phys. Scr.* **95**(1), 015502 (2019)
- Kassa-Baghdouche, L., Cassan, E.: High efficiency slotted photonic crystal waveguides for the determination of gases using mid-infrared spectroscopy. *Instrum. Sci. Technol.* **46**(5), 534–544 (2018)
- Kassa-Baghdouche, L., Boumaza, T., Bouchemat, M.: Planar photonic crystal nanocavities with symmetric cladding layers for integrated optics. *Opt. Eng.* **53**(12), 127107 (2014)
- Kassa-Baghdouche, L., Boumaza, T., Cassan, E., Bouchemat, M.: Enhancement of Q-factor in SiN-based planar photonic crystal L3 nanocavity for integrated photonics in the visible-wavelength range. *Optik* **126**(22), 3467–3471 (2015)
- Kassa-Baghdouche, L., Boumaza, T., Bouchemat, M.: Optimization of q-factor in nonlinear planar photonic crystal nanocavity incorporating hybrid silicon/polymer material. *Phys. Scr.* **90**(6), 065504–065511 (2015)

- Kassa-Baghdouche, L., Boumaza, T., Bouchemat, M.: Optical properties of point-defect nanocavity implemented in planar photonic crystal with various low refractive index cladding materials. *Appl. Phys. B* **121**(3), 297–305 (2015)
- Kraeh, C., Martinez-Hurtado, J., Popescu, A., Hedler, H., Finley, J.J.: Slow light enhanced gas sensing in photonic crystals. *Opt. Mater.* **76**, 106–110 (2018)
- Lai, W.C., Chakravarty, S., Wang, X., Lin, C., Chen, R.T.: On-chip methane sensing by near-IR absorption signatures in a photonic crystal slot waveguide. *Opt. Lett.* **36**(6), 984–986 (2011)
- Lalanne, P., Sauvan, C., Hugonin, J.P.: Photon confinement in photonic crystal nanocavities. *Laser Photonics Rev.* **2**(6), 514–526 (2008)
- Li, K., Li, J., Song, Y., Fang, G., Li, C., Feng, Z., Su, R., Zeng, B., Wang, X., Jin, C.:  $L_n$  slot photonic crystal microcavity for refractive index gas sensing. *IEEE Photonics J.* **6**(5), 1–9 (2014)
- Lin, H., Luo, Z., Gu, T., Kimerling, L.C., Wada, K., Agarwal, A., Hu, J.: Mid-infrared integrated photonics on silicon: a perspective. *Nanophotonics* **7**(2), 393–420 (2017)
- Liu, Y., Saleemink, H.: Photonic crystal-based all-optical on-chip sensor. *Opt. Express* **20**(18), 19912–19920 (2012)
- Liu, Q., Tian, H., Yang, D., Zhou, J., Yang, Y., Ji, Y.: Nanoscale radius-graded photonic crystal sensor arrays using interlaced and symmetrical resonant cavities for biosensing. *Sens. Actuators, A* **216**, 223–230 (2014)
- Mandelstam, V.A., Taylor, H.S.: Harmonic inversion of time signals and its applications. *J. Chem. Phys.* **107**(17), 6756–6769 (1997)
- Maza, D.C., Garcia, D.S., Deriziotis, I., Rodriguez, A., Llorca, J.: Macroporous silicon filters, a versatile platform for ndir spectroscopic gas sensing in the MIR. *J. Electrochem. Soc.* **166**(12), B1010–B1015 (2019)
- Oskooi, A.F., Roundy, D., Ibanescu, M., Bermel, P., Joannopoulos, J.D., Johnson, S.G.: MEEP: a flexible free-software package for electromagnetic simulations by the FDTD method. *Comput. Phys. Commun.* **181**(3), 687–702 (2010)
- Qian, X., Zhao, Y., Zhang, Y., Wang, Q.: Theoretical research of gas sensing method based on photonic crystal cavity and fiber loop ring-down technique. *Sens. Actuators B: Chem.* **228**, 665–672 (2016)
- Rajasekar, R., Robinson, S.: Nano-electric field sensor based on two dimensional photonic crystal resonator. *Opt. Mater.* **85**, 474–482 (2018)
- Rajasekar, R., Robinson, S.: Nano-pressure and temperature sensor based on hexagonal photonic crystal ring resonator. *Plasmonics* **14**(1), 3–15 (2019)
- Siraji, A.A., Zhao, Y.: High-sensitivity and high-Q-factor glass photonic crystal cavity and its applications as sensors. *Opt. Lett.* **40**(7), 1508–1511 (2015)
- Sünner, T., Stichel, T., Kwon, S.H., Schlereth, T., Höfling, S., Kamp, M., Forchel, A.: Photonic crystal cavity based gas sensor. *Appl. Phys. Lett.* **92**(26), 261112 (2008)
- Vakili, M., Noori, M.: A highly accurate refractive index sensor with two operation modes based on photonic crystal ring resonator. *Ann. Phys.* **531**(7), 1800453 (2019)
- Wang, X., Lv, J., E, S., Han, B., Zhang, Y.N.: Theoretical design and simulation optimization of photonic crystal cavity for tetrahydrofuran vapor sensing. *physica status solidi (b)* **256**, 1900221 (2019)
- Yoshie, T., Scherer, A., Hendrickson, J., Khitrova, G., Gibbs, H., Rupper, G., Ell, C., Shchekin, O., Deppe, D.: Vacuum Rabi splitting with a single quantum dot in a photonic crystal nanocavity. *Nature* **432**(7014), 200–203 (2004)
- Zhang, Y., Zhao, Y., Wang, Q.: Multi-component gas sensing based on slotted photonic crystal waveguide with liquid infiltration. *Sens. Actuators B: Chem.* **184**, 179–188 (2013)
- Zhang, Y., Zhao, Y., Wang, Q.: Measurement of methane concentration with cryptophane E infiltrated photonic crystal microcavity. *Sens. Actuators B: Chem.* **209**, 431–437 (2015)
- Zhao, Y., Zhang, Y., Lv, R., Li, J.: Electric field sensor based on photonic crystal cavity with liquid crystal infiltration. *J. Lightwave Technol.* **35**(16), 3440–3446 (2017)
- Zhou, J., Huang, L., Fu, Z., Sun, F., Tian, H.: Multiplexed simultaneous high sensitivity sensors with high-order mode based on the integration of photonic crystal  $1 \times 3$  beam splitter and three different single-slot PCNCs. *Sensors* **16**(7), 1050 (2016)